ISSN 1674-1056
http://cpb.iphy.ac.cn
http://iopscience.iop.org/cpb
中国物理 B
Chinese Physics
中国物理
Chinese Physics B

Current-phase relations of a ring-trapped Bose-Einstein condensate with a weak link

Xiu-Rong Zhang(张秀荣), Wei-Dong Li(李卫东)

Citation: Chin. Phys. B . 2019, 28(1): 010303. **doi:** 10.1088/1674-1056/28/1/010303
Journal homepage: http://cpb.iphy.ac.cn; http://iopscience.iop.org/cpb

What follows is a list of articles you may be interested in

Sonic horizon dynamics of ultracold Fermi system under elongated harmonic potential

Ying Wang(王颖), Shuyu Zhou(周蜀渝)
Chin. Phys. B . 2018, 27(10): 100312. **doi:** 10.1088/1674-1056/27/10/100312

Topologically protected edge gap solitons of interacting Bosons in one-dimensional superlattices

Xi-Hua Guo(郭西华), Tian-Fu Xu(徐天赋), Cheng-Shi Liu(刘承师)
Chin. Phys. B . 2018, 27(6): 060307. **doi:** 10.1088/1674-1056/27/6/060307

Moving bright solitons in a pseudo-spin polarization Bose-Einstein condensate

Tian-Fu Xu(徐天赋), Yu-Feng Zhang(张玉峰), Lei-Chao Xu(许磊超), Zai-Dong Li(李再东)
Chin. Phys. B . 2017, 26(10): 100304. **doi:** 10.1088/1674-1056/26/10/100304

Inverse problem of quadratic time-dependent Hamiltonians

Guo Guang-Jie, Meng Yan, Chang Hong, Duan Hui-Zeng, Di Bing
Chin. Phys. B . 2015, 24(8): 080301. **doi:** 10.1088/1674-1056/24/8/080301

Application of the homotopy analysis method for the Gross-Pitaevskii equation with a harmonic trap

Shi Yu-Ren, Liu Cong-Bo, Wang Guang-Hui, Zhou Zhi-Gang
Chin. Phys. B . 2012, 21(12): 120307. **doi:** 10.1088/1674-1056/21/12/120307

Current–phase relations of a ring-trapped Bose–Einstein condensate with a weak link*

Xiu-Rong Zhang(张秀荣) and Wei-Dong Li(李卫东)†

Institute of Theoretical Physics and Department of Physics, State Key Laboratory of Quantum Optics and Quantum Optics Devices, Collaborative Innovation Center of Extreme Optics, Shanxi University, Taiyuan 030006, *China*

(Received 5 October 2018; revised manuscript received 26 October 2018; published online 30 December 2018)

The current–phase relations of a ring-trapped Bose–Einstein condensate interrupted by a rotating rectangular barrier are extensively investigated with an analytical solution. A current–phase diagram, single and multi-valued relation, is presented with a rescaled barrier height and width. Our results show that the finite size makes the current–phase relation deviate a little bit from the cosine form for the soliton solution in the limit of a vanishing barrier, and the periodic boundary condition selects only the plane wave solution in the case of high barrier. The reason for multi-valued current–phase relation is given by investigating the behavior of soliton solution.

Keywords: ring-trapped Bose–Einstein condensate, weak link, current–phase relation, analytical solution

PACS: 03.75.Lm, 47.37.+q, 74.50.+r **DOI:** 10.1088/1674-1056/28/1/010303

1. Introduction

The current–phase relation plays an important role to explore the basic properties and their applications for superfluids or superconductors with a weak link.[1–3] While it is not easy to implement this relationship in superconductor or superfluid circuits,[4–6] some recent experimental progress[5,7–12] has been made towards realizing a ring-type trap and a repulsive rotating barrier (weak link) for ultra-cold atoms, which have inspired relative investigations. In particular, the current-phase relations were experimentally measured in Ref. [12].

Although extensive theoretical works have been done on this ring-trapped Bose–Einstein condensate (BEC) system,[13–23] there is little analytical investigation that has explored its properties in depth. In Ref. [24], the analytical solutions were used to describe the phase transitions by changing the strength of interaction or the frequency of rotation in a homogeneous ring trapped BEC. The current–phase relations of a BEC through a static barrier were analytically studied in Ref. [6], by considering an open boundary condition and an infinity size.

Novel phase transitions have been predicted in Ref. [25], with the help of an analytical solution for the ring-trapped BEC with a rotating weak link. A parity symmetry breaking between two topological phase states was suggested by changing the barrier height V crossing a critical value V_c. Meanwhile, a discontinuous phase transition was predicted through hysteresis with changing the velocity of the barrier. Meanwhile, the current–phase relations of this system have not yet been investigated.

In this manuscript, we will explore the properties of the current–phase relations of a ring-trapped BEC interrupted by a rotating rectangular barrier with the analytical solutions in Ref. [25]. The effects of the periodic boundary condition and the finite size of the ring on the current–phase relations will be discussed. A new current–phase diagram is presented with rescaled barrier height and width. Finally, a reasonable reason for understanding the experimental linear current–phase relation reported in Ref. [12] is given.

2. Model and stationary solutions

We consider a ring-trapped BEC at ultra-low temperature stirred by a rotating barrier with the velocity v, similarly with experimental cases in Refs. [11] and [12]. This problem can be well-described by the one-dimensional Gross–Pitaevskii equation (GPE) with the periodic boundary condition.[17,21–23] In the rotating frame, moving with the barrier, the 1D time-independent dimensionless GPE is

$$\left(-\frac{1}{2}\frac{\partial^2}{\partial x^2}+\mathrm{i}v\frac{\partial}{\partial x}+V(x)+\eta\,|\Psi(x)|^2\right)\Psi(x)=\mathcal{E}\Psi(x), \quad (1)$$

where the energy and length are measured in units of $\hbar^2/mL^2$ and the perimeter of the ring L, respectively. $\mathcal{E}$ is the chemical potential. In Eq. (1), the effective nonlinearity is defined as $\eta = 4\pi N a_s L$, where N is the atom number and a_s is the effective 1D s-wave scattering length. In the following, we are only concerned with the case in one period, $x \in [-1/2, 1/2]$. The barrier in the rotating frame is described as

$$V(x)=\begin{cases} V, & 0\le|x|\le d/2,\\ 0, & d/2\le|x|\le 1/2, \end{cases} \quad (2)$$

*Project supported by the National Natural Science Foundation of China (Grant No. 11874247), the National Key Research and Development Program of China (Grant Nos. 2017YFA0304500 and 2017YFA0304203), PCSIRT, China (Grant No. IRT-17R70), and the Program of State Key Laboratory of Quantum Optics and Quantum Optics Devices, China (Grant No. KF201703).

†Corresponding author. E-mail: wdli@sxu.edu.cn

© 2019 Chinese Physical Society and IOP Publishing Ltd

where $V > 0$ and d is the width of the barrier.

The wave function can be expressed as $\Psi(x) = \sqrt{\rho(x)}\,\mathrm{e}^{\mathrm{i}\theta(x)}$. Substituting this expression into Eq. (1), we get the relation between the phase $\theta(x)$ and the density $\rho(x)$

$$\theta(x) = vx + \int \frac{j}{\rho(x)}\,\mathrm{d}x, \tag{3}$$

with the current j, and the equation of $\rho(x)$ satisfying

$$2\rho\rho'' - \rho'^2 - 4j^2 - 8\eta\rho^3 - 8\,(V(x) - \mu)\,\rho^2 = 0, \tag{4}$$

where $\mu = \mathcal{E} + v^2/2$. The density can be written in terms of Jacobi elliptical Sine function, such as $\rho(x) = A + A_1\,\mathrm{SN}^2(kx + \delta, m)$,[26–28] where the parameter m is the function of the unknown parameters A, k, and j. For given V, v, and η, the current j and unknown parameters (A, k, and δ) can be numerically found by considering the continuity, periodic boundary, and normalization conditions for the density. More details can be found in the Supplemental Material of Ref. [25]. With these parameters, we find all possible stationary solutions, the plane wave solutions (PW) and the soliton solutions (SL), and we can then study the relationship between the current (j) and the phase difference (γ), defined in Eq. (6).

First, it is helpful to note that the periodic boundary condition for the phase $\theta(x)$ is $\theta(1/2) - \theta(-1/2) = 2\pi\ell$, where ℓ is the winding number. Considering Eq. (3), the periodic boundary condition can be explicitly written as

$$v + \int_{-1/2}^{1/2} \frac{j}{\rho(x)}dx = 2\pi\ell. \tag{5}$$

It should be pointed out that the parameters v and ℓ do not appear in other conditions mentioned above but only in the periodic boundary condition (5). So, if $\rho(x)$ is the stationary solution for given v and ℓ, then it will also be the solution for $v' = v + 2n\pi$ and $\ell' = \ell + n$, where n is an arbitrary integer. Therefore, we have a period-like structure for μ with respect to v and ℓ, shown in Fig. 1. To compare with the existing (theoretical[6] and experimental[12]) results, we have introduced two quantities, $\mu_0 = \eta$ and $\xi_0 = 1/\sqrt{2\mu_0}$, which stand on the chemical potential and the corresponding healing length for PW solution with $V = 0$, $v = 0$, and $\ell = 0$. In the following calculation, we re-scale the height (V), the value of μ, and the width (d) of barrier with μ_0 and ξ_0, respectively.

As shown in Fig. 1, there exist two kinds of stationary solutions, which are called PW and SL solutions in Ref. [25], for a given winding number ℓ. Wherein, the PW solutions for $\ell = 0$ (solid lines) can be found in a lager range for $|v| \le v_{\mathrm{c1}}$, while the SL solutions (dashed lines) can only survive for $v_{\mathrm{c}} \le |v| \le v_{\mathrm{c1}}$. The value of v_{c1} can be reduced to $v_{\mathrm{c}} = \pi$ (in our case) by increasing the barrier height to V_{c}, which indicates a continuous phase transition in Ref. [25]. For $\ell = 0$ state, when increasing the barrier velocity from zero to v_{c1}, the PW state is driven to a higher energy state (larger value of μ) along the black solid curve with triangles, and will suddenly drop to a lower energy state with $\ell = 1$, along the dash-dotted arrow line in Fig. 1. This kind of transition is suggested as one kind of discontinuous phase transition in Ref. [25]. By decreasing the barrier velocity to $v = 2\pi - v_{\mathrm{c1}}$, the PW state with $\ell = 1$ will be driven inversely along the red solid line with circles, and then jump to the lower energy state with $\ell = 0$. This finishes one complete hysteresis process, as experimentally reported in Refs. [11] and [12]. Therefore, the range between v_{c} and v_{c1} denotes the area of hysteresis, which has been experimentally proven by adjusting the barrier height V in Refs. [11] and [12], and explained theoretically in Ref. [25].

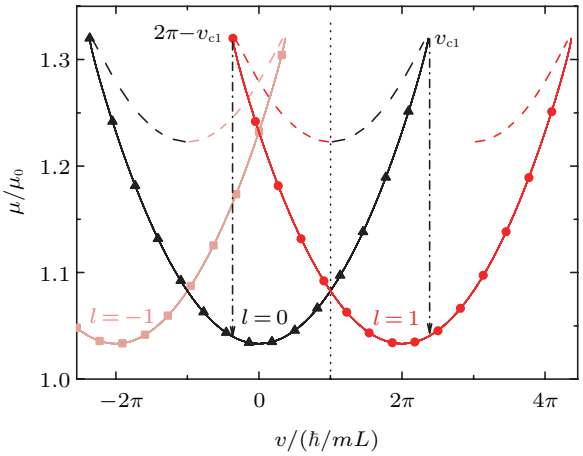


Fig. 1. The relation between μ and v with $V = 0.7\mu_0$, $\eta = 100$, $d = 0.05 \approx 0.7\xi_0$, and various winding numbers ℓ. The values of μ for PW solutions are plotted in solid lines with symbols, while those for SL solutions are plotted in dashed lines. The dash-dotted arrow lines indicate the discontinuous phase transition between two states with $\ell = 0$ and $\ell = \pm 1$.

3. Current–phase relation

The current–phase relation plays an important role in understanding the properties of this system. This offers a good opportunity to explore more details on this relation with the help of all possible obtained stationary solutions (PW and SL). Some phase profiles, defined by Eq. (3), have been plotted in Fig. 2 with various rotating velocity v. Starting from $v = 0$, PW solutions have the zero current and zero phase difference. With increasing v, BECs get a negative current, which means it flows along the opposite direction with rotating barrier. In this way, a phase difference is accumulated by different ways on the two sides of the barrier. This phase difference for PW solution increases monotonously with increasing v. On the other hand, the behavior of the phase difference for SL solution is quite different and will decrease from π with increasing v from v_{c}. A simple monotonous decreasing behavior can be found for a narrow barrier ($d < 9.2\xi_0$, see Fig. 2(a) and Fig. 3), and more complex one for a wide barrier ($d > 9.2\xi_0$, see Fig. 2(b) and Fig. 4). In Fig. 2(a) ($d \sim \xi_0$), a monotonous decreasing behavior can be read from the black solid curve ($v = v_{\mathrm{c}}$), the

red dashed line ($v = 6.5 < v_{c1} \approx 7.43$) to the green dash-dotted line ($v = v_{c1}$) with increasing v, and finally the phase profile of SL solution matching with the one for PW solution at $v = v_{c1}$. While, in Fig. 2(b) ($d = 20\xi_0$), the phase difference is increasing firstly from the black solid curve ($v = v_c$) to the blue dotted line ($v = 48.5 < v_{c1} \approx 49.94$), and then decreasing to the green dash-dotted line ($v = v_{c1}$). So for SL solutions, the phase difference does not show monotonous relation with v (this can also be seen in the following current–phase relation).

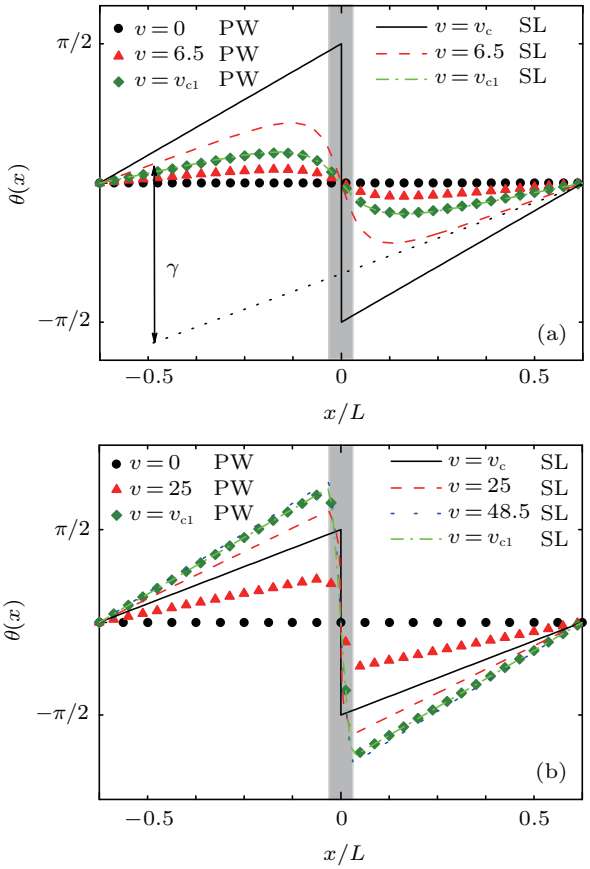


Fig. 2. Examples of the phase profiles for $\ell = 0$ and various velocity v with $V = 0.7\mu_0$, $\eta = 100$, $d = 0.05 \approx 0.7\xi_0$ in panel (a) and $V = 0.6\mu_0$, $\eta = 80000$, $d = 0.05 = 20\xi_0$ in panel (b). The grey region is the position of the barrier.

In Ref. [6], under the open boundary condition, the phase difference is defined by renormalizing the phase difference accumulated between the boundaries $x = \pm\infty$ with the one by the a plane wave with the same boundary conditions in absence of a barrier. A finite size and periodic boundary condition, in the ring-trapped BEC system, make this definition does not work. Inspired by Ref. [12], our phase difference, shown as an arrow in Fig. 2(a), is defined as the intercept difference between two tangent lines at $x = \pm 1/2$ of the phase profile. Considering the phase definition (3) and the geometrical relationship, the phase difference can be explicitly written as[25]

$$\gamma = 2\pi\ell - \left[v + \frac{j}{\rho(1/2)}\right]. \tag{6}$$

It is easy to see that the current–phase relations performs a periodic behavior with different ℓ due to the periodic boundary condition (5). In the following, we will focus on the case of $\ell = 0$.

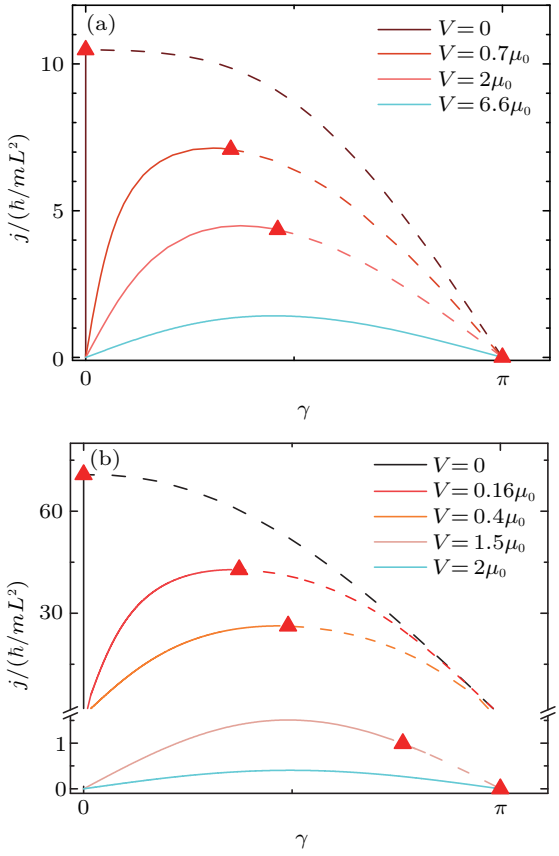


Fig. 3. The current–phase relations for various barrier height V with $\eta = 100$ and $d = 0.05 \approx 0.7\xi_0$ in panel (a), and $\eta = 5000$ and $d = 0.05 = 5\xi_0$ in panel (b). Here the current–phase relations for PW solutions are plotted in solid lines, while the current–phase relations for SL solutions are plotted in dashed lines. Red triangles indicate the positions of (γ_{c1}, j_{c1}).

Following Ref. [6], a clear relationship between the current j and the phase difference γ (defined by Eq. (6)) can be explored with re-scaled V with μ_0, and d with healing length ξ_0. A simple monotonous (single value) behavior of PW and SL solutions has been shown in Fig. 3 with narrow barriers (a) with $d \approx 0.7\xi_0$ and (b) with $d = 5\xi_0$; while, a complex one (multi-value) is in Fig. 4 with a wider barrier $d = 20\xi_0$. In Figs. 3 and 4, each curve $j(\gamma)$ constitutes with solid (PW) and dashed (SL) lines, corresponding to a given barrier height (V). The match point of PW and SL is denoted as (γ_{c1}, j_{c1}) (red triangles in Figs. 3 and 4), which indicates a kind of discontinuous phase transition at $v = v_{c1}$.[25] It is easy to see that the match point (γ_{c1}, j_{c1}) is not the maximum one in the current–phase curve, different from the case of Ref. [6].

By increasing V for a given η, the values of j_{c1} and v_{c1} will decrease. In the limit of high barriers, where a few times of μ_0 are considered in Fig. 3 and Fig. 4 (see the cyan solid lines), only PW solution survives with $j_{c1} = 0$ and $\gamma_{c1} = \pi$, where $v_{c1} = v_c$ and the hysteresis disappears. It is because

that the periodical condition does not allow SL solution exist under this condition, different from Ref. [6]. Meanwhile, the current–phase relation for PW solution, now satisfies a sinusoidal form, $j \propto \sin(\gamma)$, and was called the one in Josephson regime in Ref. [6]. Furthermore, a finite size effect can be easily read from the limit of vanishing barrier $V = 0$. Increasing the value of nonlinear parameter η is equivalent with increasing the size L compared with ξ_0. In our case, this means that $L = 14\xi_0$ in Fig. 3(a), $L = 100\xi_0$ in Fig. 3(b), and $L = 400\xi_0$ in Fig. 4. The relation of $j \propto \cos(\gamma/2)$ for SL solution, can be numerically proved for large size in Figs. 3(b) and 4, similar to Ref. [6], but a deviation from the cosine form can be found in Fig. 3(a).

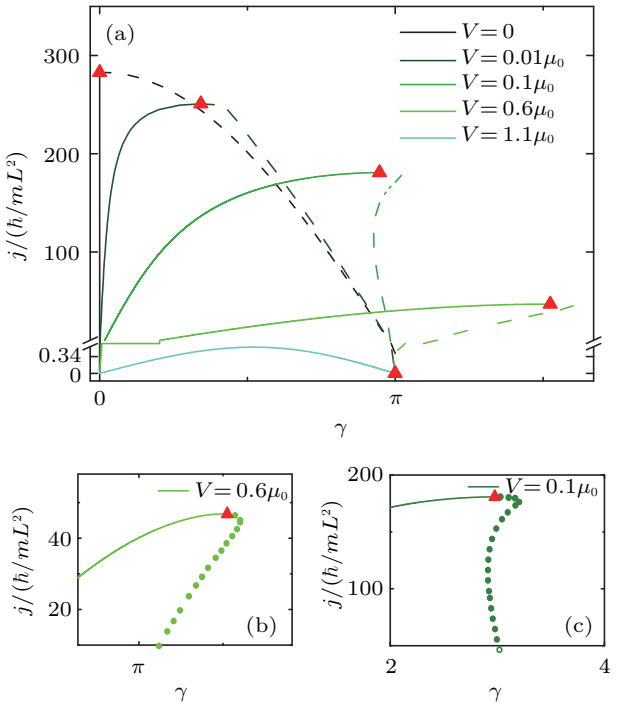


Fig. 4. The current–phase relations for various barrier height V with $\eta = 80000$ and $d = 0.05 = 20\xi_0$. The curves in panels (b) and (c) show more details about type I and type II of multi-valued current–phase relations. Here, the current–phase relations for PW (SL) solutions are plotted in solid (dashed) lines. The red triangles have the same meaning as those in Fig. 3.

The reason for the multi-valued situation, which is also called as re-entrant current–phase relation,[6] is due to the SL solution. Once the barrier is wide enough, in our case $d > 9.2\xi_0$ (see the blue and yellow regions in Fig. 5), a soliton is localized completely within the barrier. As suggested in Ref. [6], the phase accumulated from the peak of SL and from the flat tail is different. The competition between these two parts makes this kind of behavior complex. A large phase difference γ (over π) can be found only in this wide barrier. As shown in Fig. 3, two possible behaviors are found, called as Type I (Fig. 4(b)) and type II (Fig. 4(c)). For Type I, the curve may have two values of j at the same γ, while it may have three values for Type II.

To show the current–phase relation more clearly, a phase diagram with the rescaled barrier height (V/μ_0) and width (d/ξ_0) is presented in Fig. 5, which is obtained by adjusting nonlinear parameter η (equivalent to modify d/ξ_0) and barrier height V, by keeping $d = 0.05$. A large single-valued regime is divided by a curve (blue rhombus) with $j = 0$ at $v = v_c$ for PW solution. The sinusoidal regime is also called as Josephson regime, wherein the barrier is higher. Since $v_{c1} = v_c$, the area of hysteresis is zero in this regime. It is interesting to note that its border also stands for the critical V_c in the continuous phase transition suggested in Ref. [25]. The borders of multi-valued Type I and II are simply fixed by their definitions by scanning V.

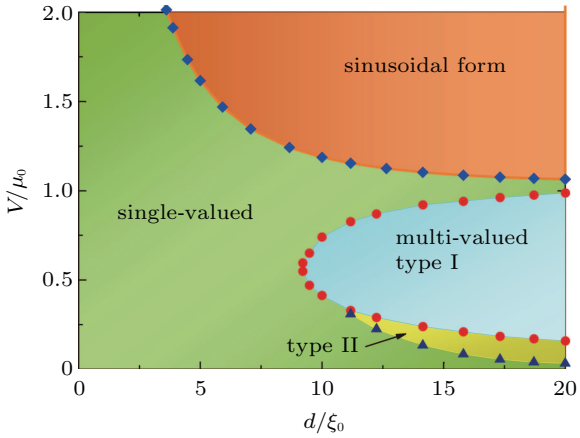


Fig. 5. The phase diagram of the current–phase relation with the ratios of V/μ_0 and d/ξ_0.

Finally, we would like to mention the comparison between our analytical results and the experimental results reported in Ref. [12], wherein a straight line relation between the current j and phase difference γ was found in the case of $d = 20\xi_0 \approx 0.04L$ and $V = 0.6\mu_0$. To compare with it,[12] we simply make $d = 0.04$, $\eta = 130000$, $V = 78000 = 0.6\mu_0$, and $\ell = 0$, which makes our system have the same conditions. Without any fitting, we plot the experimental results in Fig. 6 as light blue dots and the analytical result as a blue solid line. The obvious deviation from the experimental results can be seen. One of the reasons is the fact that the experiment is not in the one-dimensional regime and not in zero temperature. The recent experiment about the area of the hysteresis loops in the ring-trapped BEC has shown a strong temperature dependence.[29] Lower temperature and better consistency can be found between the experimental results and the GPE results. However, we think the loss of the total atomic number may be another reason. The loss of the atomic number means the decrease of η, because the nonlinearity η is proportional to the atomic number N. As shown by the red dashed line in Fig. 6, a proper decrease of η (about 20% considered according to the experiment[11]) is helpful to make a good agreement with the experimental data. This confirms our conjecture.

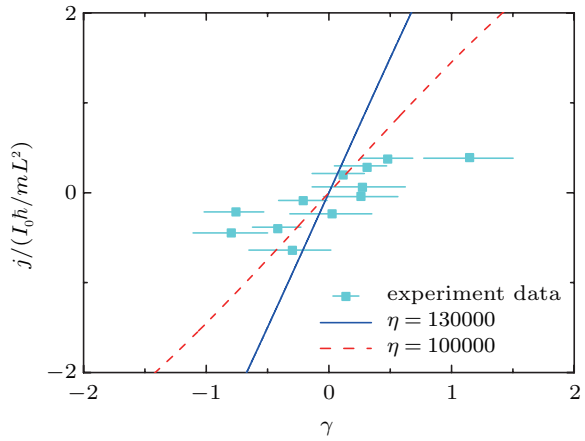


Fig. 6. Comparison with the experiment data, with $d = 0.04$, $V = 78000$, $\ell = 0$, and different η. I_0 is a constant in Ref. [12] and equals $2\pi\rho(1/2)$ in our case.

4. Conclusion

With the help of analytical solutions of the one-dimensional Gross–Pitaevskii equation of a ring-trapped BEC flowing through a rotating rectangular barrier, its current–phase relations $j(\gamma)$ are extensively investigated. The hysteresis in Refs. [11] and [12] can be understood in the point of view of analytical solutions. The phase diagram for the current–phase relations are shown with the ratios of V/μ_0 and d/ξ_0. Except for the normal Josephson regime, more interesting regimes, such as single and multi-valued region, are explored. Some special features induced by the periodic boundary condition and finite size are pointed out. For example, the periodic boundary condition makes only PW solution survival and the hysteresis disappears once V is large enough. Finally, the good consistency with the experimental results after considering the loss of atomic number hints that our analytical results may play a crucial role to understand the relative experimental results.

Acknowledgment

The authors would like to thank Francesco Piazza and Augusto Smerzi for helpful discussion.

References

[1] Packard R E and Vitale S 1992 *Phys. Rev. B* **46** 3540
[2] Schwab K, Bruckner N and Packard R E 1997 *Nature* **386** 585
[3] Simmonds R W, Marchenkov A, Hoskinson E, Davis J C and Packard R E 2001 *Nature* **412** 55
[4] Hoskinson E, Sato Y, Hahn I and Packard R E 2006 *Nat. Phys.* **2** 23
[5] Wright K C, Blakestad R B, Lobb C J, Phillips W D and Campbell G K 2013 *Phys. Rev. Lett.* **110** 025302
[6] Piazza F, Collins L A and Smerzi A 2010 *Phys. Rev. A* **81** 033613
[7] Leggett A J 2006 *Quantum Liquids* (NewYork: Oxford University)
[8] Ramanathan A, Wright K C, Muniz S R, Zelan M, Hill W T, Lobb C J, Helmerson K, Phillips W D and Campbell G K 2011 *Phys. Rev. Lett.* **106** 130401
[9] Ryu C, Blackburn P W, Blinova A A and Boshier M G 2013 *Phys. Rev. Lett.* **111** 205301
[10] Murray N, Krygier M, Edwards M, Wright K C, Campbell G K and Clark C W 2013 *Phys. Rev. A* **88** 053615
[11] Eckel S, Lee J G, Murray N, Clark C W, Lobb C J, Phillips W D, Edwards M and Campbell G K 2014 *Nature* **506** 200
[12] Eckel S, Jendrzejewski F, Kumar A, Lobb C J and Campbell G K 2014 *Phys. Rev. X* **4** 031052
[13] Piazza F, Collins L A and Smerzi A 2009 *Phys. Rev. A* **80** 021601(R)
[14] Mathey A C, Clark C W and Mathey L 2014 *Phys. Rev. A* **90** 023604
[15] Piazza F, Collins L A and Smerzi A 2011 *New J. Phys.* **13** 043008
[16] Piazza F, Collins L A and Smerzi A 2013 *J. Phys. B* **46** 095302
[17] Cominotti M, Rossini D, Rizzi M, Hekking F and Minguzzi A 2014 *Phys. Rev. Lett.* **113** 025301
[18] Roussou A, Tsibidis G D, Smyrnakis J, Magiropoulos M, Efremidis N K, Jackson A D and Kavoulakis G M 2015 *Phys. Rev. A* **91** 023613
[19] Yakimenko A I, Bidasyuk Y M, Weyrauch M, Kuriatnikov Y I and Vilchinskii S I 2015 *Phys. Rev. A* **91** 033607
[20] Kunimi M and Kato Y 2015 *Phys. Rev. A* **91** 053608
[21] Mateo A M, Gallemi A, Guilleumas M and Mayol R 2015 *Phys. Rev. A* **91** 063625
[22] Syafwan M, Kevrekidis P, Paris-Mandoki A, Lesanovsky I, Kruger P, Hackermuller L and Susanto H 2015 arXiv:1512.07924 [cond-mat.quant-gas]
[23] Li Y, Pang W and Malomed B A 2012 *Phys. Rev. A* **86** 023832
[24] Kanamoto R, Carr L D and Ueda M 2008 *Phys. Rev. Lett.* **100** 060401
[25] Zhang X R, Piazza F, Li W D and Smerzi A 2016 *Phys. Rev. A* **94** 063601
[26] Li W D 2006 *Phys. Rev. A* **74** 063612
[27] Li W D and Smerzi A 2004 *Phys. Rev. E* **70** 016605
[28] Zhang X R and Li W D 2015 *Chin. Phys. B* **24** 070311
[29] Kumar A, Eckel S, Jendrzejewski F and Campbell G K 2017 *Phys. Rev. A* **95** 021602